

## Effect of indium composition ratio on solution-processed nanocrystalline InGaZnO thin film transistors

Gun Hee Kim, Byung Du Ahn, Hyun Soo Shin, Woong Hee Jeong, Hee Jin Kim et al.

Citation: *Appl. Phys. Lett.* **94**, 233501 (2009); doi: 10.1063/1.3151827

View online: <http://dx.doi.org/10.1063/1.3151827>

View Table of Contents: <http://apl.aip.org/resource/1/APPLAB/v94/i23>

Published by the [American Institute of Physics](#).

---

### Related Articles

Spin polarization of Zn<sub>1-x</sub>CoxO probed by magnetoresistance

*Appl. Phys. Lett.* **101**, 172405 (2012)

Temperature-dependent electron transport in ZnO micro/nanowires

*J. Appl. Phys.* **112**, 084313 (2012)

Disorder induced semiconductor to metal transition and modifications of grain boundaries in nanocrystalline zinc oxide thin film

*J. Appl. Phys.* **112**, 073101 (2012)

Robust low resistivity p-type ZnO:Na films after ultraviolet illumination: The elimination of grain boundaries

*Appl. Phys. Lett.* **101**, 122109 (2012)

P-type ZnO thin films achieved by N<sup>+</sup> ion implantation through dynamic annealing process

*Appl. Phys. Lett.* **101**, 112101 (2012)

---

### Additional information on *Appl. Phys. Lett.*

Journal Homepage: <http://apl.aip.org/>

Journal Information: [http://apl.aip.org/about/about\\_the\\_journal](http://apl.aip.org/about/about_the_journal)

Top downloads: [http://apl.aip.org/features/most\\_downloaded](http://apl.aip.org/features/most_downloaded)

Information for Authors: <http://apl.aip.org/authors>

## ADVERTISEMENT



**Goodfellow**  
metals • ceramics • polymers • composites  
70,000 products  
450 different materials  
small quantities fast

[www.goodfellowusa.com](http://www.goodfellowusa.com)

# Effect of indium composition ratio on solution-processed nanocrystalline InGaZnO thin film transistors

Gun Hee Kim,<sup>1</sup> Byung Du Ahn,<sup>1</sup> Hyun Soo Shin,<sup>1</sup> Woong Hee Jeong,<sup>1</sup> Hee Jin Kim,<sup>2</sup> and Hyun Jae Kim<sup>1,a)</sup>

<sup>1</sup>*School of Electrical and Electronic Engineering, Yonsei University, 262 Seongsanno, Seodaemun-gu, Seoul 120-749, Korea*

<sup>2</sup>*Department of Materials Science and Engineering, Yonsei University, 262 Seongsanno, Seodaemun-gu, Seoul 120-749, Korea*

(Received 4 March 2009; accepted 16 May 2009; published online 8 June 2009)

The effects of the indium content on characteristics of nanocrystalline InGaZnO (IGZO) films grown by a sol-gel method and their thin film transistors (TFTs) have been investigated. Excess indium incorporation into IGZO enhances the field effect mobilities of the TFTs due to the increase in conducting path ways and decreases the grain size and the surface roughness of the films because more  $\text{InO}_2^-$  ions induce cubic stacking faults with IGZO. These structural variations result in a decrease in density of interfacial trap sites at the semiconductor-gate insulator interface, leading to an improvement of the subthreshold gate swing of the TFTs. © 2009 American Institute of Physics. [DOI: 10.1063/1.3151827]

Recently, zinc oxide (ZnO)-based materials such as ZnO,<sup>1</sup> indium zinc oxide (IZO),<sup>2</sup> and indium gallium zinc oxide (IGZO) (Ref. 3) have been investigated for as active channel layers in thin film transistors (TFTs). They are attractive owing to the high carrier mobility, low processing temperature, excellent environmental stability, and high transparency. For large area flat panel display applications, simple solution processing with high throughput and low cost is desirable for TFT array fabrication. Recently, several research groups have demonstrated sol-gel derived TFTs using ZnO,<sup>4</sup> IZO,<sup>5</sup> and IGZO<sup>6,7</sup> as active channel layers, displaying performance comparable to vacuum-processed oxide TFTs.

In a previous study, we presented solution-processed nanocrystalline (nc)-IGZO TFTs fabricated at low temperature (below 450 °C) and proposed a formation mechanism for the IGZO film from sol-gel solution.<sup>6</sup> It was suggested that an increase in the indium content of the IGZO sol-gel solution was necessary to improve the electrical performance of the TFTs. This was because it has generally been known that heavy metal indium cations share electrons in 5s orbitals and act as electron pathways contributing to an increase in carrier mobility of TFTs.<sup>8</sup> Moreover, in IGZO sol-gel solution, in-depth understanding of the chemical, structural, and electrical properties as a function of indium content is still lacking. In this article, we report on study of the chemical reactions in the IGZO solution with varying indium content, explain the structural and electrical properties of sol-gel derived IGZO films, and extend this to device performance.

A 0.5M mixture of zinc acetate dihydrate  $[\text{Zn}(\text{OAc})_2 \cdot 2\text{H}_2\text{O}]$ , gallium nitrate hydrate  $[\text{Ga}(\text{NO}_3)_3 \cdot x\text{H}_2\text{O}]$ , and indium nitrate hydrate  $[\text{In}(\text{NO}_3)_3 \cdot x\text{H}_2\text{O}]$  was used as a sol-gel precursor, dissolved in 2-methoxyethanol (2ME) and monoethanolamine with the volume ratio of 25:1, and stirred at 70 °C for 1 h to form the IGZO sol-gel solution. The mole ratio of Ga: Zn was fixed as 1:2, and that of In:Ga was varied between 1:1, 1:3, and 1:5

(i.e., the following mole ratios were prepared: In:Ga:Zn = 1:1:2, 3:1:2, and 5:1:2).

For the TFT fabrication, we used a bottom-gate and top-contact TFT structure. MoW,  $\text{SiN}_x$ , and Ta layers were used as gate electrode, gate insulator, and source and drain electrodes respectively. IGZO active channel layers ~40 nm thick with varying indium mole ratios were deposited by spin coating after filtering and then annealed at 400 °C for 3 h.

To determine the possible chemical reactions of IGZO sol-gel solutions (such as decomposition, dehydroxylation, alloy, and crystallization), thermogravimetry and differential thermal analysis (TG-DTA) were performed in an air atmosphere. The structural properties of sol-gel derived IGZO films were examined by transmission electron microscopy (TEM) and atomic force microscopy. Hall measurements were carried out to obtain electrical properties of the films using the van der Pauw configuration. The transfer curves of TFTs were measured in the dark at room temperature with a semiconductor analyzer.

Figure 1(a) shows that the first endothermic reactions were observed with large weight losses in the range 40–100 °C. We expect that the weight losses were caused primarily by low temperature solvent evaporation, and were partially due to a loss of acetic acid produced by dissociation of  $\text{Zn}(\text{OAc})_2 \cdot 2\text{H}_2\text{O}$  to zinc monoacetate  $[\text{Zn}(\text{OAc})^+]$ .<sup>9</sup> Therefore, in this temperature region, the relative difference of weight loss due to the indium mole ratio is attributed to the difference in the amount of  $\text{OAc}^-$  in the IGZO solution. In the range 100–230 °C, the nitrate-based precursors  $\text{In}(\text{NO}_3)_3 \cdot x\text{H}_2\text{O}$  and  $\text{Ga}(\text{NO}_3)_3 \cdot x\text{H}_2\text{O}$  start to decompose to  $\text{In}(\text{OH})_3$  and  $\text{Ga}(\text{OH})_3$ . Evidence for this can be seen in the small endothermic peaks in the DTA at this temperature region, because the heat flow peaks are more clearly resolved, and have greater intensities, when the  $\text{NO}_3^-$  larger. Additionally, the acetate-based precursor was completely converted to hydroxide in this temperature region. The large exothermic peaks observed around 230 °C are interpreted as the alloying of metal hydroxides to the multicomponent oxides. The weight loss that accompanies this exothermic peak corre-

<sup>a)</sup>Electronic mail: hjk3@yonsei.ac.kr.

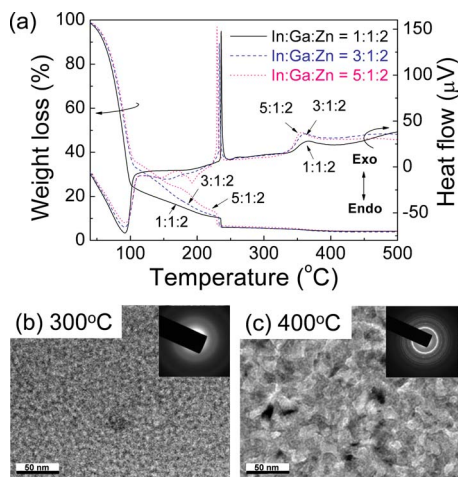


FIG. 1. (Color online) (a) TG-DTA curves of the IGZO solutions for the three different indium contents. TEM images of sol-gel derived IGZO films annealed at (b) 300 °C and (c) 400 °C and the insets show SAED patterns of the films.

sponds to dehydration of the metal hydroxides. The exothermic peaks in the DTA curves around 350 °C without weight loss, correspond to the crystallization of the IGZO.

To confirm that the peak at 350 °C corresponds to the crystallization, we conducted TEM analysis of IGZO samples extracted at 300 and 400 °C, results of which are shown in Figs. 1(b) and 1(c). No clear crystalline structure was observed in the TEM image of the sample annealed at 300 °C, implying that it was in an amorphous phase. In contrast, at 400 °C, the selected area electron diffraction (SAED) pattern shows discontinuous diffraction rings, which are attributed to the IGZO crystal and which indicate that these are polycrystalline. Based on the results, it can be convinced that the last exothermic reactions in DTA curves are strongly related to crystallization of IGZO. It was also confirmed that the nanocrystalline grains grown at 400 °C show (000 $l$ ) orientation of  $\text{InGaO}_3(\text{ZnO})_2$  by x-ray diffraction pattern (not shown in here).

Figure 2 shows plain-view TEM images of IGZO samples with (a) 1:1:2, (b) 3:1:2, and (c) 5:1:2 mole ratios, with insets showing the SAED patterns. All the samples were prepared at 400 °C. IGZO (1:1:2), IGZO (3:1:2), and IGZO (5:1:2) have grains sizes of  $\sim 27.2$ ,  $\sim 14.7$ , and  $\sim 7.6$  nm, respectively. The grain size decreased with increasing indium content. This may be related to the solubility limit, due to incorporation of indium into the IGZO. The crystallographic structure of IGZO consists of alternate stacking of  $\text{InO}_2^-$  layers and  $\text{GaO}(\text{ZnO})_m^+$  blocks. The structure of the  $\text{GaO}(\text{ZnO})_m$  blocks is very similar to that of wurtzite ZnO.<sup>8</sup> In contrast,  $\text{InO}_2^-$  has a cubic structure, and so the  $\text{In}^{3+}$  that is

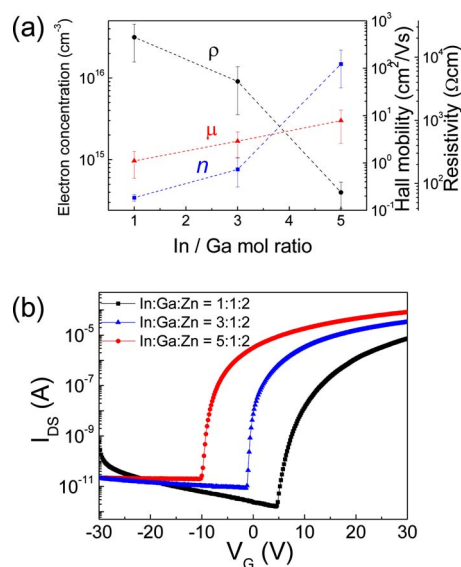


FIG. 3. (Color online) (a) Electrical characteristics of sol-gel derived IGZO films for differing indium content (b) Drain current gate-voltage transfer characteristics of  $\sim 40$  nm-thick solution-processed IGZO TFTs with  $L = 150$   $\mu\text{m}$  and  $W = 1000$   $\mu\text{m}$ .

not incorporated into the IGZO because of the solubility limit can result in the cubic stacking faults ( $\text{InO}_2^-$ ) in the IGZO.<sup>10,11</sup> This obstructs  $c$ -axis growth of IGZO resulting in a decrease of the grain size. An increase in the indium mole ratio is correlated with an increase in magnitude of the exothermic peaks corresponding to IGZO crystallization at  $\sim 350$  °C. This implies that as the indium concentration in increased, the activation energy for crystallization increases too.

The spin-coated IGZO films were prepared on the  $\text{SiN}_x$  gate insulator layer at 400 °C to investigate electrical properties as a function of indium mole ratio. From Fig. 3(a), we can see that as the indium mole ratio increases, the average electron concentration rises from  $3.43 \times 10^{14}$  to  $1.48 \times 10^{16}$   $\text{cm}^{-3}$ , and the average electrical resistivity decreases from  $2.07 \times 10^4$  to  $7.22 \times 10^1$   $\Omega \text{ cm}$ . The increase in indium mole ratio gives rise to a larger number of oxygen vacancies and zinc interstitials, which results in more free electrons.<sup>11</sup> As the indium mole ratio increases, the average Hall mobility increases from 1.11 to 7.84  $\text{cm}^2/\text{V s}$ . Excess indium that is not contained in the IGZO structure may link to indium atoms in the IGZO interlayer, providing more conducting pathways for electrons, and hence increasing the mobility. This trend has been observed in previous reports: Mobility is enhanced by increasing the carrier concentration in IZO (Ref. 12) and IGZO.<sup>13</sup> On the other hand, grain boundary scattering effect could be ignored because calculated mean-

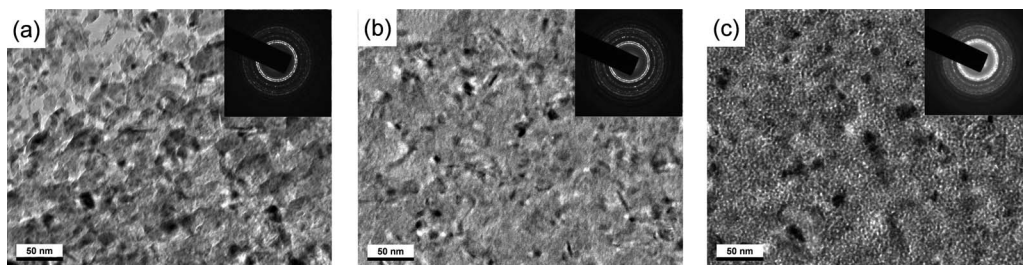


FIG. 2. TEM images and SAED patterns (inset) of sol-gel derived IGZO films for In:Ga:Zn ratios of (a) 1:1:2, (b) 3:1:2, and (c) 5:1:2.



TABLE I. Comparison of the electrical characteristics including  $\mu_{\text{FE}}$ ,  $I_{\text{on/off}}$ ,  $V_{\text{th}}$ ,  $S$ ,  $N_t$ , and rms roughness for solution-processed IGZO thin films and TFTs as a function of the indium mole ratio.

In:Ga:Zn mole ratio	$\mu_{\text{FE}}$ ( $\text{cm}^2/\text{V s}$ )	$I_{\text{on/off}}$ ratio	$V_{\text{th}}$ (V)	$S$ (V/decade)	$N_t$ ( $\text{cm}^{-2}$ )	rms roughness (nm)
1:1:2	0.56	$4.58 \times 10^6$	15.84	2.81	$5.77 \times 10^{12}$	2.26
3:1:2	0.90	$3.84 \times 10^6$	3.52	1.16	$2.31 \times 10^{12}$	1.44
5:1:2	1.25	$4.14 \times 10^6$	-5.09	1.05	$2.08 \times 10^{12}$	1.36

free paths are quite smaller than grain sizes observed in TEM images.

Figure 3(b) shows the transfer characteristics of the TFTs with solution-processed IGZO films as active channel layers for the different indium mole ratios. All the TFTs exhibit good operating performance, with on/off ratios ( $I_{\text{on/off}}$ ) of  $\sim 10^6$ . The field effect mobilities ( $\mu_{\text{FE}}$ ) of IGZO (1:1:2), IGZO (3:1:2), and IGZO (5:1:2) TFTs in the saturation region were extracted as 0.56, 0.90, and 1.25  $\text{cm}^2/\text{V s}$ , respectively. The variation of  $\mu_{\text{FE}}$  with indium mole ratio exhibits the same trend as that found in the Hall mobilities. Interestingly, the transfer curves are shifted in the negative direction; that is,  $V_{\text{th}}$  decreases from 15.84 to -5.09 V as the indium mole ratio is increased. This is almost certainly due to the increase in the number of free electrons associated with the increasing indium content. From the transfer characteristics, we estimate the gate voltage swing,  $S$ , through the relation<sup>12</sup>

$$S = \frac{dV_G}{d(\log I_D)}.$$

$S$  values of 2.81, 1.16, and 1.05 V/decade were obtained for IGZO (1:1:2), IGZO (3:1:2), and IGZO (5:1:2) TFTs, respectively. We can also infer the maximum density of the surface states ( $N_t$ ) at the interface between the IGZO channel layer and the  $\text{SiN}_x$  gate insulator layer the using following equation:<sup>12</sup>

$$N_t = \left( \frac{S \log(e)}{\frac{kT}{q}} - 1 \right) \frac{C_i}{q}.$$

Table I summarizes electrical characteristics of the TFTs and the root-mean-square (rms) roughness as a function of the indium mole ratio. In general, the roughness and density of the film were directly connected with  $N_t$ . As the rms roughness value increases, more carriers become trapped in defect sites, and we see a corresponding increase in  $N_t$ . This results in reduction of the gate voltage swing,  $S$ .<sup>14</sup> The decrease in the grain size caused by the additional indium incorporated into the IGZO reduces the surface roughness, thereby decreasing  $N_t$ , increasing  $S$ , and improving the electrical performance of the transistor.

In summary, we have synthesized the precursor solutions for deposition of IGZO films, and solution-processed the IGZO films into active channel layers in TFTs, with varying indium mole ratios. The results show that the excess indium affects the crystal growth of IGZO and leads to a decrease in the grain size and surface roughness, improving  $S$  value of the TFTs because of the reduced trap density. Indium 5s orbital sharing also increased the field effect mobility,  $\mu_{\text{FE}}$ , and the on current of TFTs. We have shown that optimized indium content in solution-processed IGZO TFTs can provide significant improvements in the performance of these transistors.

This work was supported by the Korea Science and Engineering Foundation (KOSEF), grant funded by the Korean government (MOST) (Grant No. R0A-2007-000-10044-0).

- <sup>1</sup>E. M. C. Fortunato, P. M. C. Barquinha, A. C. M. B. G. Pimentel, A. M. F. Gonçalves, A. J. S. Marques, R. F. P. Martins, and L. M. N. Pereira, *Appl. Phys. Lett.* **85**, 2541 (2004).
- <sup>2</sup>N. L. Dehuff, E. S. Kettenring, D. Hong, H. Q. Chiang, J. F. Wager, R. L. Hoffman, C. H. Park, and D. A. Keszler, *J. Appl. Phys.* **97**, 064505 (2005).
- <sup>3</sup>K. Nomura, H. Ohta, A. Takagi, T. Kamiya, M. Hiromichi, and H. Hosono, *Nature (London)* **432**, 488 (2004).
- <sup>4</sup>B. S. Ong, C. Li, Y. Li, Y. Wu, and R. Loutfy, *J. Am. Chem. Soc.* **129**, 2750 (2007).
- <sup>5</sup>D. H. Lee, Y. J. Chang, G. S. Herman, and C. H. Chang, *Adv. Mater. (Weinheim, Ger.)* **19**, 843 (2007).
- <sup>6</sup>G. H. Kim, H. S. Shin, B. D. Ahn, K. H. Kim, W. J. Park, and H. J. Kim, *J. Electrochem. Soc.* **156**, H7 (2009).
- <sup>7</sup>G. H. Kim, H. S. Kim, H. S. Shin, B. D. Ahn, K. H. Kim, and H. J. Kim, *Thin Solid Films* **517**, 4007 (2009).
- <sup>8</sup>H. Hosono, *J. Non-Cryst. Solids* **352**, 851 (2006).
- <sup>9</sup>S. Bandyopadhyay, G. K. Paul, R. Roy, S. K. Sen, and S. Sen, *Mater. Chem. Phys.* **74**, 83 (2002).
- <sup>10</sup>T. Kamiya, Y. Takeda, K. Nomura, H. Ohta, H. Yanagi, M. Hirano, and H. Hosono, *Cryst. Growth Des.* **6**, 2451 (2006).
- <sup>11</sup>B. Kumar, H. Gong, and R. Akkipeddi, *J. Appl. Phys.* **97**, 063706 (2005).
- <sup>12</sup>R. Martins, P. Barquinha, I. Ferreira, L. Pereira, G. Goncalves, and E. Fortunato, *J. Appl. Phys.* **101**, 044505 (2007).
- <sup>13</sup>A. Takagi, K. Nomura, H. Ohta, H. Yanagi, T. Kamiya, M. Hirano, and H. Hosono, *Thin Solid Films* **486**, 38 (2005).
- <sup>14</sup>J. H. Jeong, H. W. Yang, J. S. Park, J. K. Jeong, Y. G. Mo, H. D. Kim, J. Song, and C. S. Hwang, *Electrochem. Solid-State Lett.* **11**, H157 (2008).